19. Cohen, D., Chumakov, I. & Weissenbach, J. *Nature* **366,** 698–701 (1993).
20. Stevanovic, M., Lovell-Badge, R., Collignon, J. & Goodfellow, P. N. *Hum. molec. Genet.* **2,** 2013–2018 (1993).
21. Wright, E. M., Snopek, B. & Koopman, P. *Nucleic Acids Res.* **21,** 744 (1993).
22. Farr, C. J. *et al. Mamm. Genome* **4,** 577–584 (1993).
23. Schilham, M. W., van Eijk, M., van de Wetering, M. & Clevers, H. C. *Nucleic Acids Res.* **21,** 2009 (1993).
24. Mitchell, P. J. & Tjian, R. *Science* **245,** 371–378 (1989).
25. Hoefnagel, D., Wurster-Hill, D. H., Dupree, W. B., Benirschke, K. & Fuid, G. L. *Clin. Genet.* **13,** 489–499 (1978).
26. Dillon, N. & Grosveld, F. *Curr. Opin. Genet. Dev.* **5,** 260–264 (1994).
27. Capel, B. *et al. Nature Genet.* **5,** 301–307 (1993).
28. Tommerup, N. *J. med. Genet.* **30,** 713–727 (1993).
29. Mansour, S. thesis, Univ. London (1994).
30. Bianchine, J. W., Risemberg, H. M., Kanderian, S. S. & Harrison, H. E. *Lancet* **I,** 1017–1018 (1971).
31. Thurmon, T. F., DeFraites, B. S. & Anderson, E. E. *J. Pediatr.* **83,** 841–843 (1973).
32. Lynch, S. A., Gaunt, M. L. & Minford, A. M. *J. med. Genet.* **30,** 683–686 (1993).
33. Parkhurst, S. M. & Meneely, P. M. *Science* **264,** 924–932 (1994).
34. Bridge, J. *et al. Am. J. med. Genet.* **21,** 225–229 (1985).
35. Harley, V. R. *et al. Science* **255,** 453–456 (1992).
36. Denny, P., Swift, S., Connor, F. & Ashworth, A. *EMBO J.* **11,** 3705–3712 (1992).
37. van de Wetering, M., Oosterwegel, M., van Norren, K. & Clevers, H. *EMBO J.* **12,** 3847–3854 (1993).
38. Lenzini, E. *et al. Ann. Genet.* **31,** 175–180 (1988).
39. Foster, J. W. & Graves, J. A. *Proc. natn. Acad. Sci. U.S.A.* **91,** 1927–1931 (1994).
40. Buehr, M., Gu, S. & McLaren, A. *Development* **117,** 273–281 (1993).
41. Wheater, P. R., Burkitt, H. G. & Daniels, V. G. *Functional Histology* (Churchill Livingstone, Edinburgh, 1979).
42. Boehnke, M., Lange, K. & Cox, D. R. *Am. J. hum. Genet.* **49,** 1174–1188 (1991).
43. Riley, J. *et al. Nucleic Acids Res.* **18,** 2887–2890 (1990).
44. Black, D. M., Nicolai, H., Borrow, J. & Solomon, E. *Am. J. hum. Genet.* **52,** 702–710 (1993).

ACKNOWLEDGEMENTS. J.W.F., M.A.D.-S. and S.G. contributed equally to this work. We thank E. Hatchwell, S. Youings, N. Dennis, D. Donnai, C. Garrett, C. Hall, I. Moore, R. Mueller, R. Scott, J. Tolmie and R. Winter for patient samples and clinical details; H. Lehrach, H. Hummerich, D. L. Simmons, I. Kerr and the HGMP Resource Centre for libraries and clones; E. Solomon for hybrid DNAs; R. Critcher, P. Thomas and E. Rossi for *in situ* hybridizations; S. Marc and G. Casey for help in obtaining markers; G. Camerino and R. Lovell-Badge for discussion; D. Spillett and M. Walter for radiation hybrids; and P. Koopman and E. Wright for communication of results before publication and for discussion. This work was supported by the Wellcome Trust (J.W.F., P.A.W., A.J.S., P.N.G.), a Human Frontier Science Programme Organization Fellowship (M.A.D.-S.), the Medical Research Council (P.N.G.), the European Community (J.W., P.N.G.), the European Community SCIENCE Programme (S.G.), the University of Nottingham Medical School (J.D.B.), and a Peterhouse Research Studentship (C.K.).

A high-resolution image of atomic hydrogen in the M81 group of galaxies

M. S. Yun*†, P. T. P. Ho* & K. Y. Lo‡

* Harvard-Smithsonian Center for Astrophysics, 60 Garden Street, Cambridge, Massachusetts 02138, USA
† California Institute of Technology, Robinson 105-24, Pasadena, California 91125, USA
‡ Astronomy Department, University of Illinois, Urbana, Illinois 61801, USA

It has long been recognized that interactions between galaxies are important in determining their evolution. The distribution of gas—out of which new stars are formed—is strongly affected; in particular, gas may be concentrated near the nucleus, leading to a burst of star formation[1–4]. Here we present a map of atomic hydrogen (H I) in the nearest interacting group of galaxies (that dominated by M81), obtained by combining 12 separate fields observed with the Very Large Array. The H I that surrounds M81, M82 and NGC3077 (the most prominent galaxies in the group) is dominated by filamentary structures, clearly demonstrating the violent disruption of this system by tidal interactions. These observations should have detected all H I complexes more massive than 10^6 solar masses, meaning that our map contains all structures that might evolve into new dwarf galaxies.

With the Very Large Array (VLA) in the most compact D configuration, four fields centred around M82 were observed (3 h per field) on 24 and 25 January 1990, and eight additional fields including M81 and NGC3077 were observed (2 h per field) on 29 April and 1 May 1991, using all 27 telescopes. The achieved angular resolution of ~1 arcmin corresponds to a resolution of ~1 kpc at the systemic distance of 3.6 Mpc (ref. 5). Quasars 3C48 and 3C286 were used to set the flux-density scale and to calibrate the instrumental response across the bandpass of 5.125 MHz. The VLA calibrator 0831 + 557 was also observed to calibrate short-term variations of the system performance. With a spectral resolution of 48.8 kHz (10.3 km s^{-1}), we covered the full velocity range (~600 km s^{-1}) of the entire map by shifting the centre of our spectral window accordingly.

Figure 1 shows the H I distribution in the M81 group; this H I image of the 150 kpc region is at 1-kpc spatial resolution. The comparison of the H I and the optical images shows that although this system is a favourite testing ground for the density-wave theory and disk dynamics[6], active Seyfert nuclei[7,8], as well as starburst activities[9], little sign of tidal interactions can be seen in the optical image. Previous H I studies have suggested tidal interactions[10–17]. The remarkable result here is the extensive array of filamentary tidal features threading all three galaxies, dominating the H I distribution. Each galaxy has a concentration of gas surrounding it, with the 'south tidal bridge' connecting M81 and NGC3077, and the 'north tidal bridge' connecting NGC3077 and M82. This is the first time that the north tidal bridge is traced in its full extent. The physical properties of the main H I features are summarized in Table 1. We will now discuss our observations of the various features found in the H I and optical maps.

TABLE 1 Observed properties for the main H I features of the M81 group

Feature	N_{HI} (10^{21} cm^{-2})	M_{HI} ($10^9 M_\odot$)	M_{HI}(ADS) ($10^9 M_\odot$)	ΔV (km s^{-1})
M81	10.6 ± 0.2	2.63 ± 0.52	2.19 ± 0.22	30–45
M82	10.3 ± 0.2	0.75 ± 0.15	0.72 ± 0.07	40–140
NGC3077	10.7 ± 0.2	0.65 ± 0.13	1.00 ± 0.10	30–40
Concentration I	7.8 ± 0.2	0.29 ± 0.06	0.20 ± 0.05*	45–100
Concentration II	5.1 ± 0.2	0.24 ± 0.05	—	25–30†
South tidal bridge	2.4 ± 0.2	0.24 ± 0.05	—	10–30
North tidal bridge	1.6 ± 0.2	0.19 ± 0.04	—	20–30

Symbols used: N_{HI}, H I column density; M_{HI}, total H I mass; M_{HI}(ADS), total H I mass within the Holmberg radius measured with a 76-m telescope (angular resolution $\theta \approx 4$ arcmin) by Appleton, Davies and Stephenson[15]; ΔV, linewidth, full-width at half-maximum.
* H I mass estimated for Ho IX by Appleton, Davies and Stephenson[15].
† Two separate velocity components seen, each with $\Delta V \approx 25$–30 km s^{-1} (80–140 km s^{-1}, full-width at zero intensity).

M81. In the optical image, M81 appears to be a two-arm spiral. In the inner disk, the H I spiral arms trace the optical arms very closely. Moving beyond the optical disk, more H I arms can be seen which appear to be less tightly wound. West of the nucleus, one of the H I arms appears to wrap around to the east connecting with concentration I. East of the nucleus, two H I arms seem to continue on as two long spirals over 180° in angular extent, with the inner one continuing onto the south tidal bridge. The H I kinematics are shown in Fig. 2. Within the central 20 arcmin (20 kpc) around M81, the kinematics (the regular spider-like pattern for the isovelocity contours) show circular rotation. That the contours become progressively further apart away from the nucleus, shows differential rather than rigid-body rotation, that is, rotation is slower further out. This drop-off in circular rotation velocity with radius, also known as a rotation curve, was studied by Kent[18]. He found that the mass of the large bulge and the disk alone is sufficient to reproduce the observed rotation out to a radius R of 20 kpc (the only system in his sample of 16

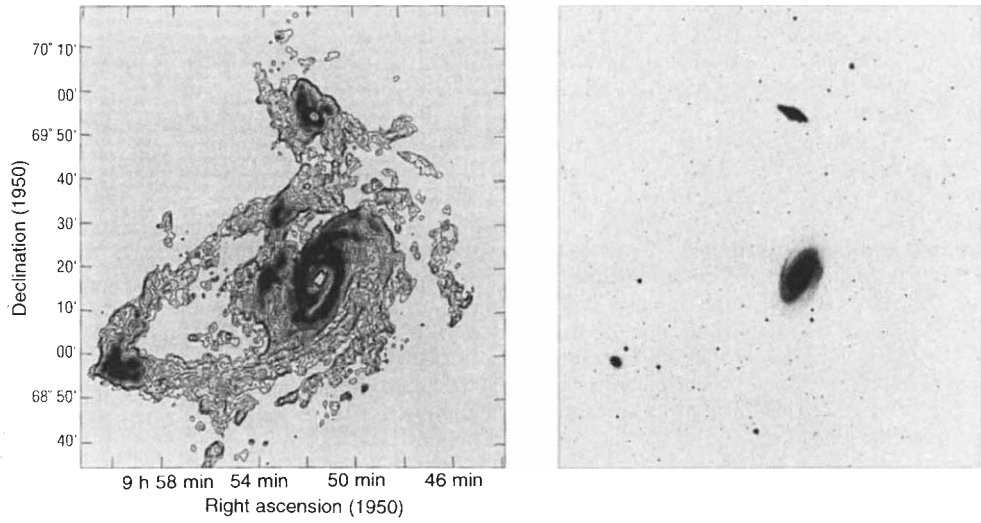

FIG. 1 Right, Palomar sky survey image (in the red band) of M81 triplet. Going from north (top) to south (bottom), the three galaxies are M82, M81 and NGC3077. Other than the optical filaments seen along the minor axis of M82, there is little hint of unusual activities in these galaxies in stellar light. Left, Integrated H I map of M81 group from the new D-array VLA mosaic observations (angular resolution $\theta = 62 \times 56$ arcsec). The mosaic of the data from 12 individual fields is made by noise-weighted linear averaging of the deconvolved (CLEANed) channel maps after removing the continuum emission and correcting for the primary beam response. Although the VLA cannot sample large structures because the interferometer resolves them, nearly all the flux from single-dish studies[15] is nevertheless recovered. The data cube contains a total of 81 channels covering the velocity range of -338 to $+486$ km s^{-1}. By overlapping adjacent fields at half-beam spacings, we achieved uniform r.m.s. noise of 0.8 mJy per beam over the sampled region. Galactic H I emission is present in three channels centred at $V_{LSR} = +12$ km s^{-1} and two channels near $V_{LSR} = -50$ km s^{-1}, where V_{LSR} is velocity with respect to the local standard of rest: for the analysis of H I emission associated with the M81 group, these channels were clipped at the 10 mJy per beam level to remove the Galactic contribution. The linear grey-scale represents the integrated H I flux. The contours correspond to the H I column density of 1.8×10^{20} cm^{-2} times 1, 2, 3, 4, 6, 10, 15, 25 and 40. A total of $5.2 \times 10^9 M_\odot$ of H I is detected. The H I structures of interest are: the north tidal bridge between M82 and NGC3077, the south tidal bridge between M81 and NGC3077, concentration I and II which are the dark knots 10 arcmin east and 20 arcmin northeast of M81 nucleus.

galaxies which may not require any dark matter to explain the observed rotation). Our new H I data show that the rotation velocity does not fall off fast enough, flattening near $R \approx 25$ kpc. Additional mass, perhaps in the form of a dark halo, is needed to keep the observed motions gravitationally bound. Figures 1 and 2 show that beyond 30 arcmin (30 kpc), the kinematics will be affected by interactions with M82 and NGC3077. The outer velocity patterns no longer behave as if they are extensions of the contours within the central 20 arcmin. This is most obvious for the southern and northern tidal bridges, hence justifying their names. We note that the outer Lindblad resonance for M81 is located at $R \approx 15$ kpc (refs 19–21). The outer H I arms are thus most likely tidally driven transient spiral features[22]. Detailed numerical simulations are needed to see if the morphology and kinematics can be produced by an interaction model.

Compared with the earlier H I studies of M81 by Gottesman and Weliachew[19], and Rots and Shane[23], the H I distribution in our study is traced much further out (>30 kpc in radius) because of the multiple pointings with better sensitivity. "Concentrations I and II", the H I complexes previously identified[19] as extragalactic, are now located inside the H I disk of M81. An exponential disk with a scale length of 10 kpc can model the radial surface density distribution well out to 40 kpc radius. A significant excess found at $R \geq 40$ kpc where M82 and NGC3077 are located, suggests that the H I of these galaxies dominates beyond this radius. There appears to be additional H I features located outside the mapped area, that is, the westernmost feature of the M81 disk is the tip of another H I streamer pointing southwest[24].

The high velocity trough and Ho IX. In the inner 25 kpc, the most significant deviation from the differential disk rotation in M81 is a ~20-kpc-long strip 10 arcmin east and northeast of the nucleus. This is seen as the Ω-shaped twists in the isovelocity contours in Fig. 2, with redshifts along the minor axis of up to 200 km s^{-1} with respect to the systemic velocity of M81 ($V = -15$ km s^{-1}). We call this the 'high velocity trough' (HVT). The associated H I mass is $3.3 \times 10^8 M_\odot$, mostly in concentration I, and the associated (lower-limit) energy and momentum are 7.4×10^{55} erg and $5.0 \times 10^{10} M_\odot$ km s^{-1}. The most likely explanation may be that these are the remnants of the recent collision

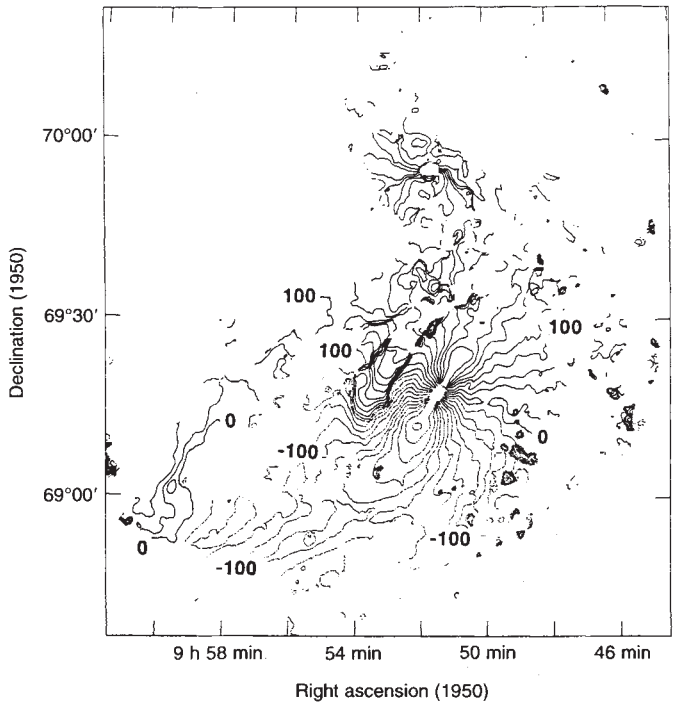

FIG. 2 Intensity-weighted mean velocity (first moment) map of H I in the M81 group. Contours are at 20 km s^{-1} intervals, and negative velocities are marked in dotted lines. The unit of the velocity label is km s^{-1}. The isovelocity contours looking like 'spider arms' centred on M81 are the classical signatures of differential rotation. This, plus the motion of the tidally disrupted H I disk in M82, accounts for the north–south velocity gradient of this system. The differential rotation for the M81 disk appears regular for the inner 20 kpc, but the twisting isovelocity contours in the outer regions (for example, the south tidal bridge) suggest significant non-circular motions at larger radii.

between M81 and M82. The velocity of M82 matches the velocity perturbation associated with HVT both in sign and magnitude. The disk orbital period at 15-kpc radius is 5×10^8 yr, and the extent of the HVT suggests that M82 passed through the western disk of M81 near $R \approx 15$ kpc some 2×10^8 yr ago. In this scenario, the Magellanic-type dwarf Ho IX found 10 arcmin east of M81, concentration I, and the $10^6 M_\odot$ molecular complex found near the H I peak[25], can be explained as the resultant stellar and gaseous debri.

Arp ring and concentration II. The main body of the Arp ring[26], a faint halo-like optical structure found just north of M81, in fact coincides with the outer H I arm of M81. Concentration II is the brightest H I complex in the tidal bridge between M81 and M82 (Fig. 1), and it coincides with the brightest optical segment of the Arp ring. The high H I column density in this direction is due to the fact that this is the site where the tidally stripped gas from M81, the tidal streamer from M82, and the north tidal bridge intersect, each with distinct velocities and velocity widths. The Arp ring may not be a single cohesive feature.

NGC3077 and tidal bridges. The north and south tidal bridges could be interpreted as a single continuous 100-kpc-long tidal feature, which connects smoothly to one of the tidally induced spiral arms of M81. We find a local H I peak near the stellar nucleus of NGC3077 while the bulk of the $7 \times 10^8 M_\odot$ H I complex is displaced by ~4 kpc from the stellar peak. The H I velocity gradient across the major axis of NGC3077 is consistent with rotation. The isovelocity contours along the south tidal bridge are perpendicular to its length as expected for a tidal tail (for example, NGC7252; ref. 27), but those along the north tidal bridge, particularly near NGC3077, are along the length, as might be expected for tidally induced shearing motion, similar to that of the remnant disk around M82. This suggests that NGC3077, now appearing as a gas-poor dwarf elliptical[28–30], could have been the origin for the gas complex around NGC3077 and the north tidal bridge.

M82. Earlier low-resolution studies by Cottrell[11] and others had interpreted the north–south overall velocity gradient perpendicular to the stellar disk as that of a tidally captured H I cloud in a polar orbit. Our recent high-resolution H I study of M82 using the VLA[17] found luminous H I streamers 10–20 kpc long emerging from the warped stellar disk, and both the two-arm morphology and the smooth connection of their velocity fields onto the disk rotation are cited as the evidence for the tidal disruption of the outer H I disk of M82 by a massive companion (M81) in a polar orbit. Our study strengthens these conclusions by tracing previously discovered H I tails to greater and fainter extents (>30 kpc). The original H I disk of M82 was probably quite substantial before the tidal disruption by M81.

The synthesis of a large mosaic in H I with good angular resolution, as has been done here, can demonstrate the effect of tidal interactions on the evolution of galaxies in small groups, especially when there is little sign of close interactions in optical images. The observations presented here suggest that the presence of even a minor companion may drastically increase the apparent gaseous extent of galaxies. Further sensitive studies of other groups of galaxies will show whether the optical or H I appearances of galaxies are better indicators of the nature and history of the system. □

Received 19 July; accepted 9 November 1994.

1. Sanders, D. B. *et al. Astrophys. J.* **325,** 74–91 (1988).
2. Scoville, N. Z. & Soifer, B. T. *Massive Stars and Starburst* (ed. K. Leitherer) 233–252 (Cambridge Univ. Press, 1991).
3. Barnes, J. E. *Astrophys. J.* **331,** 669–717 (1988).
4. Barnes, J. E. & Hernquist, L. E. *Astrophys. J.* **370,** L65–L69 (1991).
5. Freedman, W. L. *et al. Astrophys. J.* **427,** 628–655 (1994).
6. Visser, H. C. D. *Structure and Properties of Nearby Galaxies* (eds Berkhuijsen E. M. & Wielebinski, R.) 105–112 (Reidel, Dordrecht, 1978).
7. Peimbert, N. & Torres-Peimbert, S. *Astrophys. J.* **245,** 845–856 (1981).
8. Wisniewski, W. Z. & Kleinmann, D. E. *Astr. J.* **73,** 866–867 (1968).
9. Rieke, G. H., Lebofsky, M. J., Thompson, R. I., Low, F. J. & Tokunaga, A. T. *Astrophys. J.* **238,** 24–40 (1980).
10. Roberts, M. S. *External Galaxies and Quasi Stellar Objects* (ed. Evans, D. S.) 12–36 (Reidel, Dordrecht, 1972).
11. Cottrell, G. A. *Mon. Not. R. astr. Soc.* **178,** 577–589 (1977).
12. Gottesman, S. T. & Weliachew, L. *Astrophys. J.* **211,** 47–61 (1977).
13. van der Hulst, J. M. *Astr. Astrophys.* **75,** 97–111 (1979).
14. Rots, A. H. *Astr. Astrophys. Suppl. Ser.* **41,** 189–209 (1980).
15. Appleton, P. N., Davies, R. D. & Stephenson, R. J. *Mon. Not. R. astr. Soc.* **195,** 327–352 (1981).
16. Cottrell, G. A. *Mon. Not. R. astr. Soc.* **174,** 455–466 (1976).
17. Yun, M. S., Ho, P. T. P. & Lo, K. Y. *Astrophys. J.* **411,** L17–L20 (1993).
18. Kent, S. M. *Astr. J.* **93,** 816–832 (1987).
19. Gottesman, S. T. & Weliachew, L. *Astrophys. J.* **195,** 23–45 (1975).
20. Lin, C. C., Yuan, C. & Shu, F. H. *Astrophys. J.* **155,** 721–746 (1969).
21. Rots, A. H. *Astr. Astrophys.* **45,** 43–55 (1975).
22. Toomre, A. & Toomre, J. *Astrophys. J.* **178,** 623–666 (1972).
23. Rots, A. H. & Shane, W. W. *Astr. Astrophys.* **45,** 25–42 (1975).
24. Appleton, P. N. & van der Hulst, J. M. *Mon. Not. R. astr. Soc.* **234,** 957–969 (1988).
25. Brouillet, N., Henkel, C. & Baudry, A. *Astr. Astrophys.* **262,** L5–L8 (1992).
26. Arp, H. *Science* **148,** 363–364 (1965).
27. Hibbard, J. E., Guhathakurta, P., van Gorkom, J. H. & Schweizer, F. *Astr. J.* **107,** 67–89 (1994).
28. Demoulin, M. *Astrophys. J.* **157,** 81–85 (1960).
29. Barbieri, C., Bertola, F. & di Tullio, G. *Astr. Astrophys.* **35,** 463–466 (1974).
30. Price, J. S. & Gullixson, C. A. *Astrophys. J.* **337,** 658–670 (1989).

ACKNOWLEDGEMENTS. NRAO and VLA are operated by Associated Universities, Inc., under cooperative agreement with the US National Science Foundation.

Superconductivity in a layered perovskite without copper

Y. Maeno*, H. Hashimoto*, K. Yoshida*, S. Nishizaki*, T. Fujita*, J. G. Bednorz† & F. Lichtenberg†‡

* Department of Physics, Hiroshima University, Higashi-Hiroshima 724, Japan
† IBM Research Division, Zürich Research Laboratory, 8803 Rüschlikon, Switzerland

FOLLOWING the discovery of superconductivity at ~30 K in $La_{2-x}Ba_xCuO_4$ (ref. 1), a large number of related compounds have been found that are superconducting at relatively high temperatures. The feature common to all of these materials is a layered crystal structure based on a perovskite template and containing planar networks of copper and oxygen. This raises the question of whether superconductivity can occur in layered perovskites that do not contain copper. To the best of our knowledge, no such material has been found to date, despite nearly a decade of searching. We describe here the discovery of superconductivity in Sr_2RuO_4, a layered perovskite isostructural with $La_{2-x}Ba_xCuO_4$ (Fig. 1). Our results demonstrate that the presence of copper is not a prerequisite for the existence of superconductivity in a layered perovskite. But the low value of the superconducting transition temperature (T_c = 0.93 K) points towards a special role for copper in the high-temperature superconductors.

The compound Sr_2RuO_4 has been known for quite some time[2]. It is the $n = 1$ member of the homologous series expressed as $Sr_{n+1}Ru_nO_{3n+1}$, of which those members with $n = 1, 2$ and ∞ have been synthesized[2,3]. Single crystals of Sr_2RuO_4 used in the present study were grown in air by a floating-zone method[4]. They are easily cleaved, yielding plate-like crystals with (001) surfaces. Electron-probe microanalysis indicated a homogeneous distribution of the metal ions within a crystal and did not detect any impurity inclusions. All the observed peaks of powder X-ray diffraction spectra on crushed crystals are consistent with a body-centred tetragonal unit cell of the K_2NiF_4 structure with lattice parameters $a = b = 0.387$ nm and $c = 1.274$ nm at room temperature, in good agreement with the previous reports[2,4].

The low-temperature measurements were performed by using ^{3}He refrigerator (Heliox, made by Oxford Instruments, Eynsham, UK). Figure 2 shows the alternating current (a.c.) suscept-

‡ Present address: VARTA Betterie AG, R and D Centre, 65779 Kelkheim, Germany.